Supplementary Information

Prediction of Ligand Modulation Patterns on Membrane Receptors via Lysine Reactivity Profiling

Ye Zhou,[ab] Zheyi Liu,[a] Jinbao Zhang,[c] Tongyi Dou,[a] Jin Chen,[a] Guangbo Ge,[ad] Shujia Zhu*[c] and Fangjun Wang*[a]

[a] CAS Key Laboratory of Separation Sciences for Analytical Chemistry, Chinese Academy of Sciences, Dalian, 116023, China. Email: wangfj@dicp.ac.cn

[b] University of Chinese Academy of Sciences, Beijing, 100049, China

[c] Institute of Neuroscience, CAS Center for Excellence in Brain Science and Intelligence Technology, Shanghai Institutes for Biological Sciences, Chinese Academy of Sciences, Shanghai, 200031, China. Email: shujiazhu@ion.ac.cn

[d] Institute of Interdisciplinary Medicine, Shanghai University of Traditional Chinese Medicine, Shanghai, 201203, China

* Corresponding Author: wangfj@dicp.ac.cn and shujiazhu@ion.ac.cn

Experimental section

Materials and Reagents

Glu-C was purchased from Roche (Mannheim, Germany). Chymotrypsin, formaldehyde (HCHO), sodium cyanoborohydride ($NaBH_3CN$), ammonium bicarbonate (NH_4HCO_3), formic acid (FA), dithiothreitol (DTT), Tris (2-carboxyethyl) phosphine hydrochloride (TCEP), iodoacetamide (IAA), phenylmethylsulfonyl fluoride (PMSF), dimethyl sulfoxide (DMSO) and guanidine were purchased from Sigma (St. Louis, MO, USA). Acetonitrile (ACN, HPLC grade) was provided from Merck (Darmstadt, Germany). Water utilized in the experiments was purified by a Milli-Q system from Millipore Company (Bedford, MA, USA). Fused silica capillary with 75 μm i.d. was provided from Polymicro Technologies (Phoenix, USA), and with 200 μm i.d. was purchased from Yongnian Optical Fiber Factory (Hebei, China). Daisogel ODS-AQ (3 μm, 120 Å) LC packing materials were purchased from DAISO Chemical CO., Ltd. (Osaka, Japan).

Preparation of recombinant human COMT and NMDA receptors

Expression and purification of human s-COMT was conducted according to the previous report[1] with slight modifications. In brief, recombinant human COMT was transformed and expressed in Escherichia coli BL21 (DE3) cells. After that, the transformed cells were induced with 1 mM isopropyl β-D-1-thiogalactopyranoside (IPTG) when the absorbance at 600 nm was around 0.6, and then grown at 37°C overnight while shaking at 200 rpm. The cells were harvested and re-suspended in 100 mM Tris-HCl (pH 8.0), 0.3 M NaCl, 1 mM EDTA, 20% glycerol (v/v), 10 mM β-mercaptoethanol, 5 mM $MgCl_2$ with lysozyme (1 mg/mL), followed by incubation on ice for 30 min and sonication, adding PMSF (0.1 M) in advance. After lysis, the cells were centrifuged at 20,000 g for 20 min at 4ºC. The supernatant was loaded on a pre-equilibrated HisTrap™ HP metal affinity column (GE Healthcare). The column was washed with at least 50 column volumes of wash buffer (100 mM $NaPO_4$ pH 8.0, 0.4 M NaCl, 20% glycerol, 10 mM β-mercaptoethanol, 5 mM $MgCl_2$, and 20 mM imidazole). Recombinant human COMT was collected using elution buffer (100 mM $NaPO_4$ pH 7.4, 0.25 M NaCl, 20% glycerol, 5 mM β-mercaptoethanol, 5 mM $MgCl_2$, and 200 mM imidazole), followed by concentration and desalting using an Amicon Ultra-15 unit. The protein concentrations were determined using the Bradford assay. COMT was stored at -80ºC until usage.

The construct was derived from the previously reported *Xenopus laevis* NMDAR K2162 construct[2, 3] and expressed in HEK293S GnTI-cells by baculovirus infection. The membrane protein was purified as previously described[2, 3]. Briefly, cells were collected 60 h post-transduction and disrupted by sonication in TBS buffer (150 mM NaCl, 20 mM Tris-HCl, pH 8.0). The membranes were re-suspended and homogenized in TBS buffer, then solubilized in TBS buffer plus 1% MNG-3, protease inhibitors, 1 mM glutamate, 1 mM glycine, and 2 mM cholesteryl hemisuccinate (CHS) for 1.5 h, 4 ℃. The soluble fraction was bound to streptactin resin and eluted with buffer containing 5mM desthiobiotin. The concentrated GluN1/GluN2B receptors were further purified by size-exclusion chromatography in a buffer composed of 400 mM NaCl, 20 mM MES pH 6.5, 1 mM n-dodecyl β-D-maltoside (DDM), 0.2 mM CHS. Peak fractions were pooled and concentrated for experimental usage. The GluN1/GluN2B receptors were stored at -80 ºC until usage.

Active dimethyl labeling of COMT and NMDA receptors

The purified COMT was diluted with phosphate buffer (50 mM, pH 7.4) to a concentration of 0.1 μg/μL, and DTT,

$MgCl_2$, and S-adenosyl-L-methionine (SAM) were added into COMT solution in order to the final concentration of 1.6 mM, 5 mM and 200 μM, respectively. The above solutions were incubated at 37°C for 20 min in the presence and absence of 500 nM tolcapone. Then, the proteins were dimethylated by adding 4 mM HCHO and $NaBH_3CN$ at 37 °C for 0.5, 2, 5, 10, 30, and 120 min, followed by quenching with addition of 100 mM NH_4HCO_3 and incubation for 20 min at 25 °C. FA was added to adjust the pH to 2-3, further terminating the labeling reaction, while denaturing the proteins. The solutions were replaced with phosphate buffer (50 mM, pH 7.8) three times with an Amicon Ultra-0.5 3k unit and digested 16 h with Glu-C at 37 °C at an enzyme to substrate ratio 1/25 (w/w).

The purified GluN1/GluN2B receptors were diluted with size-exclusion chromatography buffer (400 mM NaCl, 20 mM MES, 1 mM DDM, 0.2 mM CHS, pH 6.5) to a concentration of 0.1 μg/μL, and incubated with DMSO vehicle, 100 μM Ro25-6981, 35 μM gavestinel and 1 mM UBP710, respectively, on ice for 30 min. Reductive dimethyl labeling was performed by adding 4 mM HCHO and $NaBH_3CN$, followed by incubation at 37 °C for 10 min. The reaction was stopped by addition of 100 mM NH_4HCO_3 and a subsequent incubation for 20 min at 25 °C. Samples were filtrated using an Amicon Ultra-0.5 10k unit and washed twice with 5 M guanidine and 100 mM NH_4HCO_3 (pH 8.0). Then, the proteins were reduced with 5 mM TCEP for 20 min and alkylated with 10 mM IAA for 30 min in the dark at room temperature. After removing guanidine, the proteins were digested by chymotrypsin for 12 h at 37 °C at an enzyme to substrate ratio 1/25 (w/w).

LC-MS/MS analysis

The digested peptides were separated using in-house packed capillary column (75 μm, i.d., 15 cm length) packed with C18 particles (3 μm, 120 Å). The flow rate was 300 nL/min. The solution of 0.1% (v/v) FA/H_2O was used as mobile phase A, and 0.1% (v/v) FA/ 80% acetonitrile (ACN) was used as mobile phase B. The elution gradient executed was 8% to 45% mobile phase B lasted for 78 min.

Q-Exactive hybrid quadrupole-Orbitrap mass spectrometer (Thermo, San Jose, CA) was utilized for MS analyses. The MS parameters were set as follows: ion transfer capillary 275 °C, spray voltage 2.0 kV, full MS scan from m/z 400 to 2000 with a resolution of 70,000 (m/z 200). Data-dependent MS/MS scans were performed by selecting the 12 most intense ions in the full MS scan for higher-energy collisional dissociation (HCD) with 27% normalized collision energy. The MS/MS scans were also acquired by the Orbitrap mass analyzer with a 35,000 resolution (m/z 200), and the AGC target was set to 1×10^5 with a max injection time of 120 ms. The ions carrying charge lower than +1 or higher than +8 were excluded, and the dynamic exclusion was set as 30 s.

Data analysis

The sequence of human COMT was obtained from UniProt (http://www.uniprot.org). All of the *.raw files were converted to *.mgf files by Protein Discovery (version 1.4). The generated *.mgf files were searched against the COMT database via Mascot (version 2.3.0). Dimethylation of lysine and oxidation of methionine were set as variable modifications. Glu-C was specified as the proteolytic enzyme with up to two missing cleavages. Precursor ion mass tolerance was 10 ppm and the fragment ion mass tolerance was 0.05 Da. Peptides with Mascot score and false discovery rate (FDR) were controlled to ≥ 20 and < 0.01, respectively.

The sequences of *Xenopus laevis* GluN1/GluN2B receptors were consistent with chain A and B of 5IOU from PDB (https://www.rcsb.org). The *.raw files were processed using MaxQuant (Version 1.5.3.30, http://www.maxquant.org/). Carbamidomethyl cysteine was set as a fixed modification, and dimethylation of lysine

and oxidation of methionine were allowed as variable modifications. Chymotrypsin was specified as the proteolytic enzyme with up to four missing cleavages. Precursor ion mass tolerance was 10 ppm and the fragment ion mass tolerance was 0.05 Da. FDR for peptide and protein was controlled to < 0.01. All other parameters were the same as the default settings.

Each COMT sample was analyzed three times and each NMDAR sample was analyzed twice with an experimental replication on the MS. According to the results from Mascot and the msms files generated from MaxQuant, we calculated the lysine reactivity through spectra counts of lysine containing peptides with and without dimethyl labeling as the following method: lysine reactivity = $(N_1/N_2) \times 100\%$, where N_1 was the spectra counts of dimethyl labeled peptides; N_2 was the total spectral counts of the corresponding peptides identified by MS.[4, 5] Besides, we utilized the total spectra counts of co-characterized (peptides without lysine) as internal standard to normalize the datasets among different MS experiments. The alteration value of lysine reactivity is the difference between the lysine reactivity in the presence and absence of small-molecule ligand. The filter of alteration value in labeling reactivity > 15% and p value < 0.05 (in student ttest) was utilized to predict the lysine residues with high significance that involved into the dynamic ligand modulation processes.

The mass spectrometry datasets have been deposited to the ProteomeXchange Consortium via the PRIDE[6] partner repository with identifier PXD012222.

Circular dichroism (CD) spectroscopy.

BSA was diluted with phosphate buffer (50 mM, pH 7.4) to a concentration of 0.1 μg/μL. Reductive dimethyl labeling was performed by adding 4 mM HCHO and $NaBH_3CN$, followed by incubation at 25 °C or 37 °C for 10 min or 2h. Structural changes in five BSA samples (before and after dimethyl labeling in different conditions) were probed by CD spectroscopy. CD spectra were collected on a BioLogic MOS-450 spectropolarimeter (BioLogic, France) at room temperature. Each measurement was recorded between 190~250 nm in a 1 nm path length quartz cuvette at a scanning rate of 1 nm/s. Each scan was repeated 3 times to obtain an averaged value.

Supplementary Text

The modulation patterns of tolcapone on COMT

Catechol-O-methyltransferase (COMT) is an important enzyme in catecholamine biochemistry and pharmacology, which catalyzes the methylation of biologically active or toxic catechols.[7] COMT has been the subject of considerable research interest as it plays an important role in the pathophysiology of different human disorders including schizophrenia,[8] bipolar disorders,[9] Parkinson's disease[10] and many other diseases,[11] thus serving as drug target for neurological disorders. Two COMT inhibitor drugs, entacapone and tolcapone, have received approval by FDA and are applied in the treatment of Parkinson's disease.[10] Two identical mixtures of COMT, Mg^{2+} and SAM were incubated with and without tolcapone at 37 °C, respectively, followed with active chemical labeling and liquid chromatography-tandem mass spectrometry (LC-MS/MS) analysis.[12] The lysine reactivity with or without tolcapone incubation was systematically compared at different labeling time (0.5, 2, 5, 10, 30 and 120 min, Table S1).

The importance of lysine residues

Lysine is one of the most widely existing amino acids in proteins.[13] Lysine residues play essential roles in the regulation of proteins structure, interaction and function.[14] As the lysines are generally positively charged under their native conditions, they are located at or near the small-molecule ligand binding regions of protein complexes and play important roles in mediating protein-ligand interactions via covalent or non-covalent interactions.[15-17] The chemical reactivity of lysine residues, usually referred to the side-chain primary amino group, is mainly related to their local microenvironments, including proximal interactions,[12] steric exclusion effects[18] and exposure surfaces to water.[19] Globally profiling the reactivity and ligandability of lysine residues is promising to find the protein function sites, which could be covalently targeted by small-molecule ligands.[20] However, there are some disadvantages in conventional strategies for lysine reactivity profiling. The chemical reactions with covalent labeling reagents, such as sulfonyl fluorides[21] and vinyl sulfonamides,[22] are usually performed, which might neutralize the positive charge states of lysine residues and deactivate the proteins. Further, the reaction molecules usually contain aryl groups in order to increase the reactivity with lysines,[23] thus the lysine residues with high steric effects or strong proximal interactions are difficult to be accessed and profiled. There is still lack of a uniform chemical labeling strategy that can unbiasedly investigate lysine reactivity without inactivating proteins as well as quantitatively monitor the detailed modulation patterns of lysine residues induced by any exogenous stimulus.

REFERENCES

1. J. Y. Zhang and J. P. Klinman, *J. Am. Chem. Soc.* , 2011, **133**, 17134-17137.
2. C. H. Lee, W. Lu, J. C. Michel, A. Goehring, J. Du, X. Song and E. Gouaux, *Nature*, 2014, **511**, 191-197.
3. S. Zhu, R. A. Stein, C. Yoshioka, C. H. Lee, A. Goehring, H. S. McHaourab and E. Gouaux, *Cell*, 2016, **165**, 704-714.
4. Y. H. Feng, G. De Franceschi, A. Kahraman, M. Soste, A. Melnik, P. J. Boersema, P. P. de Laureto, Y. Nikolaev, A. P. Oliveira and P. Picotti, *Nat. Biotechnol.*, 2014, **32**, 1036-1044.
5. M. Q. Dong, J. D. Venable, N. Au, T. Xu, S. K. Park, D. Cociorva, J. R. Johnson, A. Dillin and J. R. Yates, *Science*, 2007, **317**, 660-663.
6. J. A. Vizcaino, A. Csordas, N. del-Toro, J. A. Dianes, J. Griss, I. Lavidas, G. Mayer, Y. Perez-Riverol, F. Reisinger, T. Ternent, Q. W. Xu, R. Wang and H. Hermjakob, *Nucleic Acids Res.* , 2016, **44**, D447-D456.
7. J. Zhang and J. P. Klinman, *J. Am. Chem. Soc.* , 2011, **133**, 17134-17137.
8. K. E. Lewandowski, *Harv. Rev. Psychiatry*, 2007, **15**, 233-244.
9. S. Shifman, M. Bronstein, M. Sternfeld, A. Pisante, A. Weizman, I. Reznik, B. Spivak, N. Grisaru, L. Karp, R. Schiffer, M. Kotler, R. D. Strous, M. Swartz-Vanetik, H. Y. Knobler, E. Shinar, B. Yakir, N. B. Zak and A. Darvasi, *American Journal of Medical Genetics Part B-Neuropsychiatric Genetics*, 2004, **128b**, 61-64.
10. M. J. Bonifacio, P. N. Palma, L. Almeida and P. Soares-Da-Silva, *CNS Drug Rev.* , 2007, **13**, 352-379.
11. M. C. Houston, *Altern. Ther. Health Med.*, 2007, **13**, 128-133.
12. Y. Zhou, Y. Wu, M. D. Yao, Z. Y. Liu, J. Chen, J. Chen, L. R. Tian, G. Y. Han, J. R. Shen and F. J. Wang, *Anal. Chem.* , 2016, **88**, 12060-12065.
13. H. Eagle, *Science*, 1959, **130**, 432-437.
14. S. Sokalingam, B. Madan, G. Raghunathan and S. G. Lee, *Biotechnol. Bioprocess Eng.* , 2013, **18**, 18-26.
15. R. Chowdhury, K. K. Yeoh, Y. M. Tian, L. Hillringhaus, E. A. Bagg, N. R. Rose, I. K. Leung, X. S. Li, E. C. Woon, M. Yang, M. A. McDonough, O. N. King, I. J. Clifton, R. J. Klose, T. D. Claridge, P. J. Ratcliffe, C. J. Schofield and A. Kawamura, *EMBO Rep*, 2011, **12**, 463-469.
16. R. Baron, C. Binda, M. Tortorici, J. A. McCammon and A. Mattevi, *Structure*, 2011, **19**, 212-220.
17. M. P. Martin, S. H. Olesen, G. I. Georg and E. Schonbrunn, *ACS Chem. Biol.* , 2013, **8**, 2360-2365.
18. M. K. Menon and A. L. Zydney, *J. Membr. Sci.* , 2001, **181**, 179-184.
19. S. K. Pal, J. Peon and A. H. Zewail, *Proc. Natl Acad. Sci. USA*, 2002, **99**, 1763-1768.
20. S. M. Hacker, K. M. Backus, M. R. Lazear, S. Forli, B. E. Correia and B. F. Cravatt, *Nat. Chem.*, 2017, **9**, 1181-1190.
21. Q. Zhao, X. H. Ouyang, X. B. Wan, K. S. Gajiwala, J. C. Kath, L. H. Jones, A. L. Burlingame and J. Taunton, *J. Am. Chem. Soc.* , 2017, **139**, 680-685.
22. S. Asano, J. T. Patterson, T. Gaj and C. F. Barbas, *Angewandte Chemie-International Edition*, 2014, **53**, 11783-11786.
23. D. A. Shannon, R. Banerjee, E. R. Webster, D. W. Bak, C. Wang and E. Weerapana, *J. Am. Chem. Soc.* , 2014, **136**, 3330-3333.

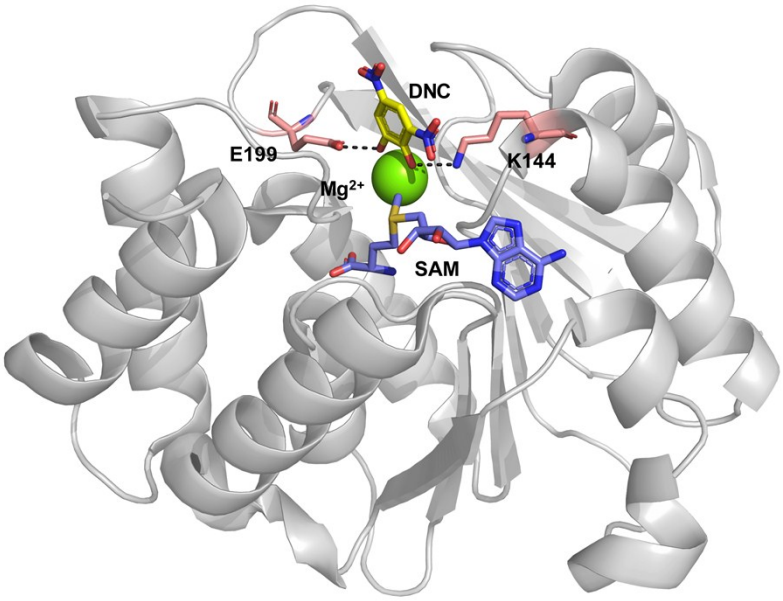

Figure S1. Schematic representation of the crystal structure of COMT. In the catalytic active conformation of COMT, two catechol hydroxyl groups form hydrogen bonds with the side chains of E199 and K144, and one of the hydroxyl group is positioned in proximity to the activated methyl group of the co-substrate SAM. The hydrogen bonds to K144 and E199 are depicted in dashed lines. SAM, DNC, Mg^{2+}, K144 and E199 are in slate, yellow, green and salmon, respectively. PDB: 3BWM.

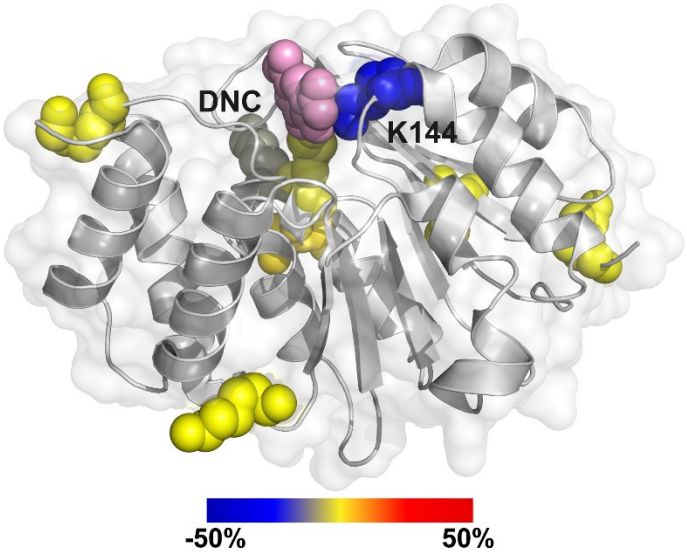

Figure S2. The modulation pattern of COMT with small-molecule inhibitor (shown as DNC, an analogue of tolcapone). DNC and lysine residues are represented in spheres. The alteration value of lysine reactivity between -50% and 50% is visualized from blue to red. PDB: 3BWM.

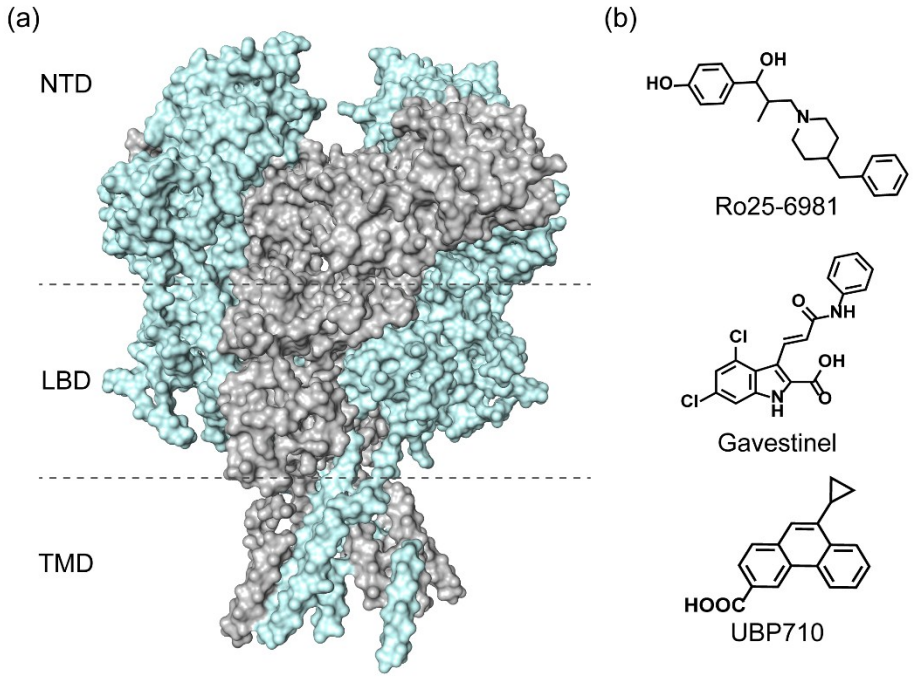

Figure S3. The structure of NMDA receptor (a) and three ligands (b) Ro25-6981, gavestinel and UBP710.

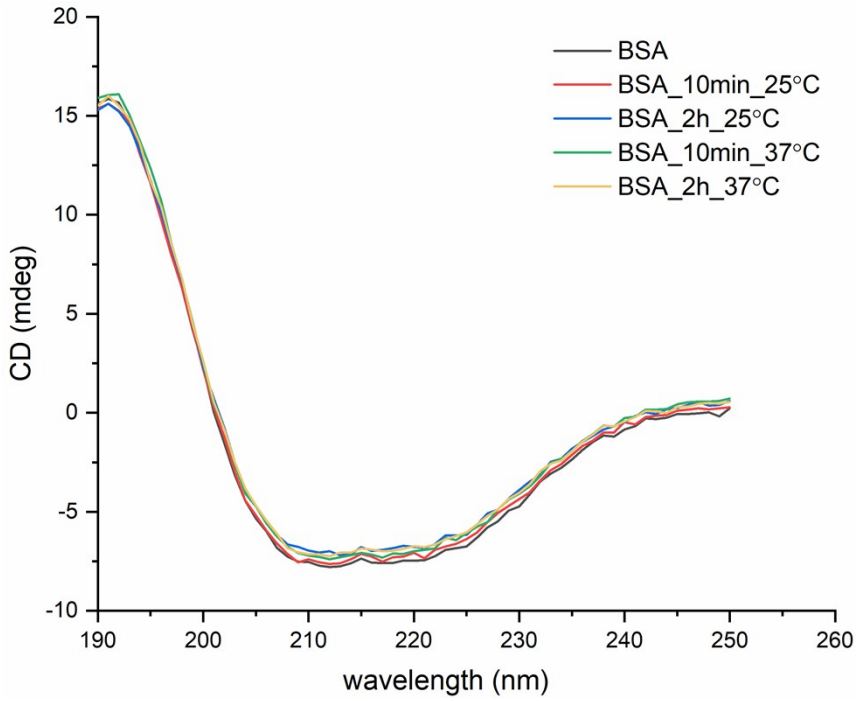

Figure S4. CD spectra of BSA before and after dimethyl labeling in different conditions.

Table S1. The labeling reactivity of lysine residues in COMT with and without tolcapone interaction at different labeling time.

Lysine	COMT without tolcapone						COMT with tolcapone						Alteration value					
	0.5 min	2 min	5 min	10 min	30 min	120 min	0.5 min	2 min	5 min	10 min	30 min	120 min	0.5 min	2 min	5 min	10 min	30 min	120 min
K36	47.80%	72.80%	79.50%	82.50%	91.90%	97.60%	51.90%	69.10%	78.40%	81.60%	83.10%	97.80%	4.10%	-3.70%	-1.10%	-0.90%	-8.80%	0.20%
K45	0.00%	16.70%	25.00%	48.30%	47.00%	73.80%	0.00%	6.70%	19.20%	19.70%	24.00%	50.70%	0.00%	-10.00%	-5.80%	-28.60%	-23.00%	-23.10%
K46	11.10%	N/A	35.70%	63.90%	81.50%	100.00%	10.30%	16.70%	43.60%	45.60%	58.00%	93.90%	-0.80%	N/A	7.90%	-18.30%	-23.50%	-6.10%
K48	58.90%	63.30%	55.70%	38.30%	55.40%	87.10%	57.90%	70.00%	79.40%	74.40%	76.70%	93.90%	-1.00%	6.70%	23.70%	36.10%	21.30%	6.80%
K109	N/A	93.30%	88.90%	100.00%	91.70%	100.00%	N/A	91.70%	80.00%	100.00%	100.00%	100.00%	N/A	-1.60%	-8.90%	0.00%	8.30%	0.00%
K144	0.00%	3.00%	4.80%	18.80%	80.10%	100.00%	0.00%	0.00%	0.00%	3.80%	12.10%	49.00%	0.00%	-3.00%	-4.80%	-15.00%	-68.00%	-51.00%
K209	0.00%	0.00%	10.90%	22.20%	43.40%	81.50%	0.00%	0.00%	0.00%	0.00%	21.80%	81.00%	0.00%	0.00%	-10.90%	-22.20%	-21.60%	-0.50%

Table S2. The labeling reactivity of lysine residues in NMDA receptors with the interaction of Ro25-6981, gavestinel and UBP710, respectively.

lysines	subunits	labeling reactivity_Control					labeling reactivity_Ro25-6981							labeling reactivity_Gavestinel							labeling reactivity_UBP710						
		1	2	3	4	mean	1	2	3	4	mean	alteration value	P value	1	2	3	4	mean	alteration value	P value	1	2	3	4	mean	alteration value	P value
K131	GluN1	31.6%	28.6%	26.1%	29.6%	29.0%	27.3%	21.7%	27.3%	25.0%	25.3%	-3.6%	0.08	27.3%	27.3%	26.3%	38.5%	29.8%	0.9%	0.79	41.9%	46.7%	56.7%	50.0%	48.8%	19.9%	0.00
K178	GluN1	0.0%	0.0%	0.0%	12.5%	3.1%	0.0%	14.3%	0.0%	0.0%	3.6%	0.4%	0.93	0.0%	0.0%	0.0%	0.0%	0.0%	-3.1%	0.36	0.0%	0.0%	0.0%	0.0%	0.0%	-3.1%	0.36
K179	GluN1	100.0%	100.0%	100.0%	100.0%	100.0%	100.0%	100.0%	100.0%	100.0%	100.0%	0.0%	N/A	100.0%	100.0%	100.0%	100.0%	100.0%	0.0%	N/A	100.0%	100.0%	100.0%	100.0%	100.0%	0.0%	N/A
K187	GluN1	85.3%	81.3%	81.3%	83.1%	82.7%	75.6%	77.0%	73.2%	75.6%	75.4%	-7.4%	0.00	76.3%	73.1%	74.7%	76.7%	75.2%	-7.6%	0.00	66.3%	71.3%	66.7%	69.0%	68.3%	-14.4%	0.00
K190	GluN1	26.5%	18.8%	24.0%	26.8%	24.0%	28.2%	24.3%	26.8%	28.2%	26.9%	2.9%	0.21	26.3%	24.4%	28.0%	26.0%	26.2%	2.2%	0.32	30.1%	31.0%	39.1%	29.6%	32.5%	8.5%	0.03
K193	GluN1	42.6%	51.3%	45.3%	42.3%	45.4%	43.6%	48.6%	39.4%	43.6%	43.8%	-1.6%	0.60	47.4%	41.0%	45.3%	41.1%	43.7%	-1.7%	0.55	49.4%	52.9%	52.2%	45.1%	49.9%	4.5%	0.15
K212	GluN1	21.1%	27.8%	22.7%	25.0%	24.1%	22.2%	33.3%	23.8%	23.8%	25.8%	1.7%	0.59	20.0%	18.8%	26.3%	23.8%	22.2%	-1.9%	0.43	25.0%	11.8%	21.1%	27.3%	21.3%	-2.9%	0.47
K233	GluN1	100.0%	100.0%	100.0%	100.0%	100.0%	100.0%	100.0%	N/A	100.0%	N/A	N/A	N/A	100.0%	100.0%	100.0%	100.0%	100.0%	0.0%	N/A	100.0%	100.0%	100.0%	100.0%	100.0%	0.0%	N/A
K316	GluN1	100.0%	100.0%	100.0%	100.0%	100.0%	N/A	100.0%	N/A	N/A	N/A	N/A	N/A	87.5%	100.0%	100.0%	100.0%	96.9%	-3.1%	0.36	85.7%	87.5%	81.8%	87.5%	85.6%	-14.4%	0.00
K322	GluN1	100.0%	100.0%	100.0%	100.0%	100.0%	N/A	0.0%	N/A	N/A	N/A	N/A	N/A	100.0%	100.0%	100.0%	100.0%	100.0%	0.0%	N/A	100.0%	100.0%	100.0%	100.0%	100.0%	0.0%	N/A
K329	GluN1	37.0%	37.9%	36.7%	35.9%	36.8%	42.7%	37.9%	38.5%	37.2%	39.1%	2.3%	0.13	38.6%	38.1%	36.0%	37.6%	37.6%	0.7%	0.34	39.2%	43.0%	40.6%	38.9%	40.4%	3.6%	0.01
K347	GluN1	57.1%	66.7%	62.5%	60.0%	61.6%	58.3%	54.5%	53.8%	60.0%	56.7%	-4.9%	0.10	42.9%	46.2%	50.0%	50.0%	47.3%	-14.3%	0.00	58.3%	46.2%	52.9%	46.7%	51.0%	-10.6%	0.02
K36	GluN1	93.0%	97.1%	89.2%	100.0%	94.8%	94.7%	92.5%	89.7%	93.8%	92.7%	-2.1%	0.44	85.7%	85.4%	83.3%	87.5%	85.5%	-9.3%	0.01	85.0%	81.4%	59.5%	63.9%	72.5%	-22.4%	0.02
K360	GluN1	93.3%	100.0%	83.9%	91.3%	92.1%	78.9%	94.1%	82.8%	96.0%	88.0%	-4.2%	0.46	72.7%	76.5%	88.0%	87.0%	81.0%	-11.1%	0.07	66.7%	76.9%	76.7%	76.0%	74.1%	-18.1%	0.00
K37	GluN1	53.5%	60.3%	56.8%	57.1%	56.9%	49.1%	50.9%	53.8%	59.4%	53.3%	-3.6%	0.22	33.3%	36.6%	33.3%	29.2%	33.1%	-23.8%	0.00	62.5%	58.1%	54.8%	55.6%	57.7%	0.8%	0.73
K378	GluN1	53.7%	52.8%	49.3%	51.7%	51.9%	52.5%	50.7%	55.7%	53.5%	53.1%	1.3%	0.41	45.9%	50.0%	49.2%	55.2%	50.1%	-1.8%	0.44	46.4%	54.4%	56.6%	46.4%	51.0%	-0.9%	0.76
K399	GluN1	50.0%	44.4%	48.7%	45.9%	47.3%	45.9%	47.4%	45.9%	42.9%	45.5%	-1.7%	0.31	40.0%	41.7%	43.2%	41.7%	41.6%	-5.6%	0.01	50.0%	52.6%	62.5%	57.5%	55.7%	8.4%	0.03
K432	GluN1	0.0%	50.0%	64.7%	50.0%	41.2%	0.0%	33.3%	75.0%	54.5%	40.7%	-0.5%	0.98	22.2%	44.4%	50.0%	50.0%	41.7%	0.5%	0.98	33.3%	53.8%	46.2%	0.0%	33.3%	-7.8%	0.69
K433	GluN1	0.0%	31.3%	35.3%	38.9%	26.4%	0.0%	0.0%	50.0%	36.4%	21.6%	-4.8%	0.77	22.2%	11.1%	45.0%	38.9%	29.3%	2.9%	0.81	0.0%	23.1%	7.7%	0.0%	7.7%	-18.7%	0.12
K463	GluN1	100.0%	100.0%	100.0%	100.0%	100.0%	100.0%	100.0%	94.4%	95.0%	97.4%	-2.6%	0.13	100.0%	100.0%	100.0%	100.0%	100.0%	0.0%	N/A	93.3%	91.7%	100.0%	100.0%	96.3%	-3.8%	0.14
K481	GluN1	44.4%	50.0%	50.0%	63.0%	51.9%	50.0%	56.5%	52.2%	53.8%	53.1%	1.3%	0.77	50.0%	50.0%	54.2%	52.2%	51.6%	-0.3%	0.95	60.9%	47.6%	57.7%	58.6%	56.2%	4.3%	0.41
K529	GluN1	100.0%	100.0%	94.7%	94.7%	97.4%	100.0%	100.0%	92.9%	88.2%	95.3%	-2.1%	0.54	100.0%	100.0%	93.3%	86.7%	95.0%	-2.4%	0.53	57.1%	66.7%	56.3%	58.8%	59.7%	-37.6%	0.00
K541	GluN1	76.2%	80.4%	96.1%	85.2%	84.5%	76.0%	80.7%	93.6%	85.7%	84.0%	-0.5%	0.94	45.3%	52.9%	50.0%	45.8%	48.5%	-36.0%	0.00	75.0%	76.6%	90.9%	86.4%	82.2%	-2.3%	0.71
K542	GluN1	83.3%	76.1%	84.3%	87.0%	82.7%	86.0%	82.5%	85.1%	89.3%	85.7%	3.0%	0.31	56.6%	54.9%	54.2%	54.2%	55.0%	-27.7%	0.00	77.1%	78.7%	68.2%	70.5%	73.6%	-9.1%	0.04
K668	GluN1	30.0%	50.0%	80.0%	100.0%	65.0%	35.2%	45.8%	63.2%	58.3%	50.6%	-14.4%	0.42	19.0%	33.3%	25.0%	41.7%	29.8%	-35.2%	0.07	33.3%	60.0%	22.2%	31.3%	36.7%	-28.3%	0.16
K675	GluN1	65.9%	68.2%	68.3%	72.2%	68.6%	63.6%	64.4%	56.3%	60.0%	61.1%	-7.6%	0.02	51.4%	48.6%	42.5%	44.4%	46.7%	-21.9%	0.00	47.8%	54.3%	35.4%	37.8%	43.8%	-24.8%	0.00
K698	GluN1	100.0%	100.0%	100.0%	100.0%	100.0%	100.0%	100.0%	N/A	N/A	N/A	N/A	N/A	100.0%	100.0%	N/A	N/A	N/A	N/A	N/A	100.0%	N/A	100.0%	100.0%	N/A	N/A	N/A
K715	GluN1	76.3%	69.4%	73.2%	73.5%	73.1%	72.7%	78.4%	71.1%	75.0%	74.3%	1.2%	0.59	52.3%	57.5%	56.5%	58.1%	56.1%	-17.0%	0.00	68.3%	68.2%	63.6%	61.4%	65.4%	-7.7%	0.01
K733	GluN1	53.2%	63.5%	61.6%	63.7%	60.5%	54.4%	57.7%	56.3%	56.9%	56.3%	-4.2%	0.15	43.0%	48.0%	45.3%	43.1%	44.8%	-15.7%	0.00	52.6%	50.5%	54.0%	53.4%	52.6%	-7.9%	0.02
K754	GluN1	100.0%	100.0%	100.0%	100.0%	100.0%	100.0%	100.0%	100.0%	100.0%	100.0%	0.0%	N/A	100.0%	100.0%	100.0%	100.0%	100.0%	0.0%	N/A	100.0%	100.0%	100.0%	100.0%	100.0%	0.0%	N/A
K768	GluN1	57.1%	69.4%	68.8%	84.6%	70.0%	62.5%	56.5%	77.4%	76.5%	68.2%	-1.8%	0.83	54.5%	45.0%	74.3%	53.1%	56.7%	-13.2%	0.17	71.9%	77.8%	64.1%	71.8%	71.4%	1.4%	0.83
K780	GluN1	37.9%	38.5%	51.5%	57.1%	46.2%	37.1%	16.7%	43.8%	44.4%	35.5%	-10.7%	0.23	25.7%	22.7%	36.1%	30.3%	28.7%	-17.5%	0.02	51.4%	56.7%	43.9%	45.0%	49.2%	3.0%	0.61

K132	GluN2B	23.3%	20.8%	22.2%	27.2%	23.4%	19.4%	21.7%	26.7%	31.6%	24.9%	1.5%	0.64	25.0%	27.0%	28.6%	30.7%	27.8%	4.5%	0.05	44.0%	43.8%	41.9%	44.3%	43.5%	20.1%	0.00
K180	GluN2B	68.3%	80.0%	85.3%	82.4%	79.0%	71.1%	71.4%	77.1%	82.1%	75.4%	-3.6%	0.46	67.5%	69.0%	81.1%	78.1%	73.9%	-5.0%	0.35	63.0%	61.4%	72.2%	66.7%	65.8%	-13.2%	0.02
K210	GluN2B	74.1%	66.3%	73.8%	70.7%	71.2%	50.6%	55.0%	58.2%	58.7%	55.6%	-15.6%	0.00	69.9%	66.2%	67.4%	67.4%	67.7%	-3.5%	0.12	66.3%	72.8%	63.6%	65.2%	67.0%	-4.2%	0.17
K216	GluN2B	100.0%	100.0%	100.0%	100.0%	100.0%	100.0%	100.0%	100.0%	100.0%	100.0%	0.0%	N/A	100.0%	100.0%	100.0%	100.0%	100.0%	0.0%	N/A	100.0%	100.0%	100.0%	93.3%	98.3%	-1.7%	0.36
K217	GluN2B	53.8%	53.8%	54.5%	57.1%	54.8%	52.6%	55.0%	50.0%	50.0%	51.9%	-2.9%	0.09	52.0%	50.0%	42.9%	41.7%	46.6%	-8.2%	0.02	47.1%	41.2%	44.4%	46.7%	44.8%	-10.0%	0.00
K229	GluN2B	23.5%	23.5%	22.2%	23.5%	23.2%	20.0%	23.5%	25.0%	23.5%	23.0%	-0.2%	0.87	26.3%	23.5%	21.1%	17.6%	22.1%	-1.1%	0.59	40.0%	37.5%	32.1%	35.5%	36.3%	13.1%	0.00
K313	GluN2B	90.0%	100.0%	66.7%	85.7%	85.6%	81.8%	75.0%	87.5%	100.0%	86.1%	0.5%	0.96	100.0%	100.0%	71.4%	100.0%	92.9%	7.3%	0.49	71.4%	70.0%	54.5%	46.2%	60.5%	-25.1%	0.04
K356	GluN2B	84.0%	91.5%	90.6%	82.2%	87.1%	85.7%	83.3%	74.2%	71.2%	78.6%	-8.5%	0.09	70.6%	88.5%	81.6%	89.3%	82.5%	-4.6%	0.39	78.1%	77.8%	59.6%	69.0%	71.1%	-15.9%	0.02
K367	GluN2B	0.0%	0.0%	0.0%	0.0%	0.0%	0.0%	0.0%	0.0%	0.0%	0.0%	0.0%	N/A	0.0%	0.0%	0.0%	0.0%	0.0%	0.0%	N/A	0.0%	0.0%	0.0%	0.0%	0.0%	0.0%	N/A
K395	GluN2B	51.5%	43.9%	60.5%	55.7%	52.9%	45.8%	61.0%	54.3%	55.4%	54.1%	1.2%	0.80	55.4%	54.3%	54.9%	55.6%	55.0%	2.1%	0.57	58.0%	53.4%	53.8%	49.3%	53.6%	0.7%	0.86
K46	GluN2B	44.6%	42.5%	47.4%	51.3%	46.4%	42.9%	40.1%	43.4%	46.1%	43.1%	-3.3%	0.19	42.0%	48.4%	48.1%	50.7%	47.3%	0.9%	0.75	44.3%	35.2%	45.7%	42.9%	42.0%	-4.4%	0.19
K478	GluN2B	100.0%	100.0%	100.0%	100.0%	100.0%	100.0%	100.0%	100.0%	100.0%	100.0%	0.0%	N/A	100.0%	93.3%	100.0%	100.0%	98.3%	-1.7%	0.36	78.6%	80.0%	58.3%	72.7%	72.4%	-27.6%	0.00
K481	GluN2B	100.0%	75.0%	100.0%	100.0%	93.8%	100.0%	100.0%	100.0%	100.0%	100.0%	6.3%	0.36	66.7%	100.0%	100.0%	100.0%	91.7%	-2.1%	0.85	78.6%	80.0%	91.7%	72.7%	80.7%	-13.0%	0.13
K482	GluN2B	85.7%	100.0%	83.3%	83.3%	88.1%	70.0%	75.0%	80.0%	100.0%	81.3%	-6.8%	0.41	88.9%	66.7%	100.0%	100.0%	88.9%	0.8%	0.93	57.1%	50.0%	58.3%	54.5%	55.0%	-33.1%	0.00
K497	GluN2B	60.0%	33.3%	55.6%	57.1%	51.5%	52.9%	52.9%	50.0%	53.8%	52.4%	0.9%	0.89	59.1%	54.5%	41.7%	58.3%	53.4%	1.9%	0.80	60.0%	54.5%	70.0%	71.4%	64.0%	12.5%	0.14
K51	GluN2B	79.7%	79.5%	78.9%	81.9%	80.0%	68.6%	70.1%	77.4%	79.6%	73.9%	-6.1%	0.07	70.1%	77.4%	73.4%	78.4%	74.8%	-5.2%	0.04	76.2%	68.8%	72.1%	69.8%	71.8%	-8.2%	0.00
K587	GluN2B	23.1%	25.9%	36.7%	37.5%	30.8%	29.6%	26.9%	33.3%	38.7%	32.1%	1.4%	0.77	27.3%	28.6%	30.8%	25.0%	27.9%	-2.9%	0.48	38.5%	35.7%	37.5%	28.6%	35.1%	4.3%	0.36
K607	GluN2B	33.3%	66.7%	66.7%	100.0%	66.7%	50.0%	66.7%	66.7%	50.0%	58.3%	-8.3%	0.58	60.0%	50.0%	75.0%	66.7%	62.9%	-3.8%	0.81	40.0%	33.3%	40.0%	40.0%	38.3%	-28.3%	0.08
K612	GluN2B	100.0%	100.0%	100.0%	100.0%	100.0%	100.0%	100.0%	100.0%	100.0%	100.0%	0.0%	N/A	100.0%	100.0%	100.0%	100.0%	100.0%	0.0%	N/A	80.0%	100.0%	60.0%	60.0%	75.0%	-25.0%	0.04
K652	GluN2B	52.2%	50.0%	50.0%	57.1%	52.3%	52.0%	51.9%	52.6%	50.0%	51.6%	-0.7%	0.70	44.4%	46.2%	47.6%	47.6%	46.5%	-5.9%	0.02	39.3%	39.3%	38.7%	29.6%	36.7%	-15.6%	0.00
K653	GluN2B	87.0%	90.9%	77.3%	81.0%	84.0%	84.0%	77.8%	78.9%	81.8%	80.6%	-3.4%	0.35	81.5%	84.6%	85.7%	76.2%	82.0%	-2.0%	0.61	75.0%	75.0%	77.4%	70.4%	74.4%	-9.6%	0.03
K705	GluN2B	94.1%	92.9%	94.1%	100.0%	95.3%	92.3%	100.0%	100.0%	91.7%	96.0%	0.7%	0.81	82.1%	83.9%	100.0%	91.7%	89.4%	-5.9%	0.23	92.9%	100.0%	87.0%	92.6%	93.1%	-2.2%	0.51
K708	GluN2B	94.1%	92.9%	100.0%	94.1%	95.3%	69.2%	70.8%	92.3%	100.0%	83.1%	-12.2%	0.17	78.6%	80.6%	92.9%	100.0%	88.0%	-7.3%	0.22	71.4%	83.3%	56.5%	63.0%	68.6%	-26.7%	0.00
K730	GluN2B	71.4%	63.2%	67.5%	71.8%	68.5%	69.6%	72.3%	72.2%	69.2%	70.8%	2.4%	0.32	72.5%	71.1%	71.4%	65.6%	70.2%	1.7%	0.53	59.2%	56.9%	54.9%	57.4%	57.1%	-11.4%	0.00
K738	GluN2B	79.2%	72.1%	61.2%	66.7%	69.8%	72.9%	73.1%	66.0%	66.7%	69.7%	-0.1%	0.98	73.5%	74.5%	63.8%	60.5%	68.1%	-1.7%	0.75	58.1%	55.8%	58.1%	58.7%	57.7%	-12.1%	0.02
K74	GluN2B	90.5%	89.5%	79.2%	82.8%	85.5%	87.0%	90.9%	81.3%	88.9%	87.0%	1.5%	0.67	86.4%	91.3%	89.5%	93.3%	90.1%	4.6%	0.18	90.3%	75.0%	66.7%	60.0%	73.0%	-12.5%	0.13
K751	GluN2B	52.8%	65.6%	66.7%	65.9%	62.7%	63.6%	61.3%	71.1%	63.0%	64.8%	2.0%	0.63	45.2%	42.4%	68.3%	65.8%	55.4%	-7.3%	0.37	65.8%	66.7%	72.7%	68.4%	68.4%	5.7%	0.17
K756	GluN2B	80.0%	83.3%	66.7%	66.7%	74.2%	88.2%	82.4%	66.7%	66.7%	76.0%	1.8%	0.81	73.3%	73.3%	66.7%	62.5%	69.0%	-5.2%	0.35	75.0%	72.7%	73.3%	75.0%	74.0%	-0.2%	0.97
K788	GluN2B	59.1%	59.3%	57.7%	58.6%	58.7%	58.3%	51.1%	56.8%	58.9%	56.3%	-2.4%	0.24	57.6%	60.2%	64.8%	59.0%	60.4%	1.8%	0.31	54.9%	54.3%	52.1%	52.2%	53.4%	-5.3%	0.00
K87	GluN2B	52.3%	61.0%	55.1%	59.5%	57.0%	63.6%	58.8%	54.6%	56.2%	58.3%	1.3%	0.65	50.7%	55.6%	55.1%	54.6%	54.0%	-3.0%	0.24	60.4%	60.2%	54.1%	59.6%	58.6%	1.6%	0.54
K88	GluN2B	24.2%	21.3%	25.4%	23.4%	23.6%	23.5%	27.7%	21.8%	18.3%	22.8%	-0.7%	0.74	19.1%	21.5%	21.0%	24.1%	21.4%	-2.1%	0.16	28.8%	25.6%	32.2%	31.0%	29.4%	5.8%	0.01